



Adaptive Control of a 3-DOF Helicopter Under Structured and Unstructured Uncertainties

Hicham Chaoui¹  · Sumit Yadav²

Received: 18 February 2019 / Revised: 30 July 2019 / Accepted: 24 October 2019 / Published online: 1 November 2019
© Brazilian Society for Automatics–SBA 2019

Abstract

In this paper, an adaptive control strategy is presented for a three-degree-of-freedom helicopter under both structured and unstructured uncertainties. The adaptive control scheme learns online the helicopter's inverse model with a Lyapunov-based adaptation law to estimate the system's parameters. Moreover, a reference model is introduced to stabilize the helicopter at start-up and cope with unstructured uncertainties such as external disturbance. Therefore, the controller achieves accurate motion tracking in the presence of both structured uncertainties (parameters variation) and unstructured uncertainties (unknown disturbance). Unlike many controllers, the proposed adaptive control scheme's stability is guaranteed by Lyapunov direct method. The proposed controller's performance in coping with various uncertainties is highlighted in different operating conditions.

Keywords Adaptive control · Helicopters · Parameter variation · Uncertainties

1 Introduction

Unmanned aerial vehicles (UAVs) have attracted the attention of the scientific community from multiple disciplines due to their numerous applications. Their popularity has increased worldwide, including helicopters, which is mainly due to their ability to hover and maneuver in tight and dangerous places (Castaneda et al. 2016; Liu et al. 2013; Marantos et al. 2017). In these kinds of applications, a robust controller is required to cope with various uncertainties like changes in gravity, mass, inertia, and other unpredictable factors. Similar to aircrafts, helicopter motion also consists of controlling the pitch, roll, and yaw axis with only two rotors. However, the unique body structure of helicopters makes the pitch, roll, and yaw dynamics strongly coupled (Castaneda et al. 2016). Therefore, con-

trolling them is not trivial. Unlike conventional helicopters that use a single main rotor, the three-degree-of-freedom (3-DOF) helicopter uses two rotors and a suspending mass making it more fault tolerant. However, stabilizing the 3-DOF helicopter is not an easy task to undertake. It exhibits a complex nonlinear and unstable open-loop dynamics. The severe nonlinearities, coupling, varying operating conditions, structured and unstructured uncertainties, and external disturbances are among the typical challenges to be faced.

Various control approaches have been proposed for helicopters (Castaneda et al. 2016; Liu et al. 2013; Li et al. 2015b; Xian et al. 2015), including classical, robust, and adaptive control laws. Among popular methods, input–output linearization and back-stepping are used for their simplicity. However, linearization does not guarantee the stability in all operating conditions. Moreover, they suffer from sensitivity to parameter variations. The presence of high, particularly unstructured, uncertainties such as nonlinearities significantly changes the system's dynamics (Chaoui and Sicard 2012b). So, modeling the system's dynamics based on presumably accurate mathematical models cannot be applied efficiently in this case. This raises the urgency to consider alternative approaches for the control of this type of systems to keep up with their increasingly demanding design requirements. In Dube and Patel (2016), the translation dynamics

✉ Hicham Chaoui
hicham.chaoui@carleton.ca

Sumit Yadav
syadav@students.tntech.edu

¹ Intelligent Robotic and Energy Systems (IRES), Department of Electronics, Carleton University, 1125 Colonel By Dr, Ottawa, ON K1S 5B6, Canada

² Electrical and Computer Engineering, Tennessee Technological University, 220 W. 10th Street, Cookeville, TN 38505, USA

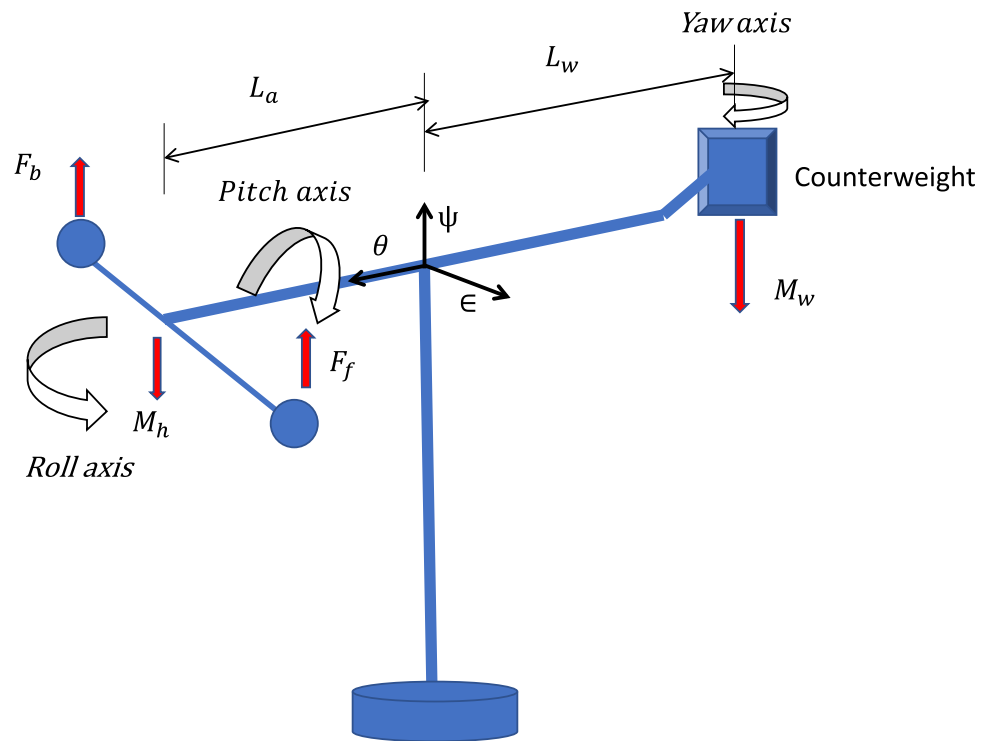
of 3-DOF helicopter is discussed with the design of adaptive control system design. The proposed control scheme is validated experimentally. In Coza and Macnab (2006), a robust adaptive fuzzy control is used for a quadrotor. A real-time stabilization control of tri-rotor with non-cyclic propellers is proposed in Cruz et al. (2008). In Tanaka et al. (2004), a robust stabilization controller is designed for RC helicopters that guarantees robust stability, good speed response, and avoidance of actuators' saturation. An adaptive fuzzy-based back-stepping control is proposed for a 3-DOF helicopter testbed with dead zone in Li et al. (2017), where fuzzy logic is used to approximate the model uncertainty and external disturbances.

A lot of research has been done on helicopters and UAVs and is still ongoing. Different control strategies are used to control helicopters. In Castaneda et al. (2016), a continuous differentiator based on adaptive second-order sliding-mode control is proposed for helicopter control. The proposed scheme combines a continuous differentiator with adaptive super twisting controllers. In Liu et al. (2013), a robust linear quadratic regulator (LQR) is used to control the altitude of a 3-DOF helicopter. In this approach, a feedback control is used for linearized approximation and a robust controller is designed to cope with uncertainties, disturbances, and other nonlinear properties. In Boby et al. (2014), a robust adaptive linear quadratic regulator (LQR) controller is designed for a 3-DOF helicopter. Results show that the integral action can eliminate the tracking errors and that the adaptive controller estimates and compensates for the uncertainty in the system. In Veeraboina and Ordonez (2018), a comparison of four different control scheme is carried out with input and output feedback linearizing (IOFL)-, direct adaptive fuzzy controller (DAC)-, linear quadratic regulator (LQR)-, and proportional integral derivative (PID)-based LQR control design. Comparison results of all four control schemes are provided. A nonlinear robust tracking control of a helicopter is proposed in Li et al. (2015b). The controller also includes a second-order auxiliary system to generate filtered error signals along with an estimator of uncertainties and disturbances. In Marantos et al. (2017), a robust control strategy is proposed to track the trajectory for small-scale unmanned helicopters. The control scheme does not depend on the explicit knowledge of the model's parameters, and each model guarantees trajectory tracking with prescribed transient and steady-state response in the presence of external disturbances. An adaptive output feedback control is used for a helicopter in Kutay et al. (2005). The adaptive control achieves adaptation to both parametric uncertainty and unmodeled dynamics and incorporates a novel approach that adapts to known actuator characteristics. In Fradkov et al. (2010), an estimator and a controller are designed for a helicopter developed at the Laboratory for Analysis and Architecture of Systems (LAAS). In here, a hybrid

continuous–discrete observation procedure is proposed for transmission of the measured data over the limited band communication channel with adaptive tuning of the coder range parameters. An adaptive back-stepping tracking control of a 6-DOF helicopter is proposed in Xian et al. (2015), where the proposed controller combines the back-stepping method with online parameters update law to achieve the control objective. In Gao and Fang (2012), another adaptive integral back-stepping control strategy proposed for a 3-DOF helicopter, the controller is capable of approximating model uncertainties online and improve the robustness of the model. Machine learning and artificial intelligence were also used to control the helicopters. In Zou and Zheng (2015), a robust adaptive radial basis function neural network is used to control the helicopter with back-stepping as the main control framework, which is amplified by radial basis function neural networks (RBFNNs) to approximate the unmodeled dynamics. An adaptive neural fault-tolerant controller of a 3-DOF helicopter is proposed in Chen et al. (2016) to cope with uncertainty and nonlinear actuator faults. A neural network disturbances observer is developed based on a radial basis function neural network, and a different nonlinear observer is also designed for the unknown external disturbances. A neural network tracking control of the 3-DOF helicopter is designed in Guo et al. (2016), with time-varying disturbances and input saturation. In Du et al. (2014), a frequency-domain system identification of an unmanned helicopter is designed based on an adaptive genetic algorithm. The model is identified based on the inputs and outputs, and then, a control compensator is designed based on the identified model. A decentralized robust second-order consensus tracking control of multiple 3-DOF helicopters using output feedback is done in Li et al. (2015a). The controller can drive the system to achieve second-order consensus tracking without measuring the velocity, so that the velocity sensor can be avoided. In Zheng and Zhong (2011), a robust attitude regulator is designed for a 3-DOF helicopter, where a linear-invariant robust controller is used to improve tracking performance. The results are validated through experiments. In Kocagil et al. (2018), a model reference adaptive control (MRAC) is designed using state-dependent Riccati equation (SDRE) for a 3-DOF helicopter.

Studies have shown that the design of robust controllers for mathematically ill-defined systems that may be subjected to structured and unstructured uncertainties is made possible with computational intelligence tools, such as artificial neural networks and fuzzy logic systems (Efe 2011; Pedro and Kala 2015; Khayamy et al. 2016). The approximation capabilities have been the main driving force behind the increasing popularity of such methods as they are theoretically capable of uniformly approximating any continuous real function to any degree of accuracy (Chaoui and Sicard

Fig. 1 3-DOF helicopter



2012a). This has led to the recent advances in the area of intelligent control (Chaoui and Gueaieb 2008; Chaoui and Sicard 2012b). Satisfactory performance is achieved with various neural network models for complex control systems (Coza and Macnab 2006; Dierks and Jagannathan 2010).

Adaptive control offers good performance in the presence of structured (parametric) uncertainties, but it falls short in the presence of unstructured uncertainties, such as disturbances. Henceforth, the contribution of this paper is to achieve motion tracking for a 3-DOF helicopter in the presence of both structured and unstructured uncertainties. The proposed control scheme combines the power of adaptive control theory against parameters variation and a reference model to cope with time-varying modeling and disturbance uncertainties. As stated earlier, conventional adaptive controllers fail to achieve robustness against both parameter uncertainties and disturbances. Thus far, very few nonlinear controllers have been proposed for the 3-DOF helicopter. Unlike many controllers, the closed-loop control scheme's stability is guaranteed by Lyapunov direct method. Furthermore, convergence analysis is also provided. The rest of the paper is organized as follows: Sect. 2 outlines the dynamic model of the helicopter. Then, the proposed adaptive control methodology is outlined in Sect. 3. In Sect. 4, numerical results are presented and discussed. Finally, we conclude with a few remarks and suggestions.

2 System Description

2.1 Dynamics

The helicopter consists of a 3-DOF rotational motion body actuated by two propellers (Rajappa et al. 2013). The two rotors provide upwards propulsion as well as direction control. The model of the system is shown in Fig. 1, which depicts the body/global coordinate systems and forces exerted on the helicopter by the counterweight and motors. The dynamic mathematical model based on Euler–Lagrange formulation is described by the following equations (Castaneda et al. 2016):

$$J_\epsilon \ddot{\epsilon} = G \cos \epsilon + L_a \cos \theta u_1 \quad (1a)$$

$$J_\psi \ddot{\psi} = L_a \cos \epsilon \sin \theta u_1 \quad (1b)$$

$$J_\theta \ddot{\theta} = L_h u_2 \quad (1c)$$

with $u_1 = F_f + F_b$, $u_2 = F_f - F_b$, $G = g(M_h L_a - M_w L_w)$, where

$M_h \in \mathbb{R}$: mass of the helicopter

$M_w \in \mathbb{R}$: mass of the counterweight

$L_a \in \mathbb{R}$: length from the rotors to the center of mass

$L_w \in \mathbb{R}$: length from the tail to the center of mass

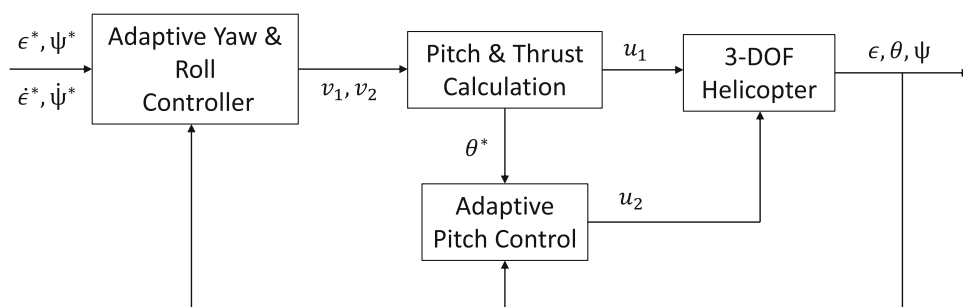
$L_h \in \mathbb{R}$: length between the rotors

$g \in \mathbb{R}$: gravitational constant

$\epsilon \in \mathbb{R}$: roll angle of the helicopter

$\psi \in \mathbb{R}$: yaw angle of the helicopter

Fig. 2 Autopilot scheme



$\theta \in \mathbb{R}$: pitch angle of the helicopter
 $u \in \mathbb{R}^2$: control input vector
 $J_\epsilon \in \mathbb{R}$: moment of inertia about roll
 $J_\psi \in \mathbb{R}$: moment of inertia about yaw
 $J_\theta \in \mathbb{R}$: moment of inertia about pitch
 F_f : front motor force
 F_b : back motor force

Before we proceed further, let us introduce the following assumptions (Castaneda et al. 2016):

- Assumption 1** The yaw and roll axes are perpendicular.
- Assumption 2** All the axes intersect in the same point, which is considered as the origin of the global coordinate frame.
- Assumption 3** The helicopter frame and counterweight mass centers are collinear with respect to the pitch axis.
- Assumption 4** The Joint friction, air resistance, and centrifugal forces are neglected.
- Assumption 5** The thrust force is proportional to the motor voltage, and motors/propellers dynamics are neglected.

Remark 1 It is noteworthy that this system is underactuated, i.e., two input forces to control three states (the yaw angle ψ , the roll angle ϵ , and the pitch angle θ).

2.2 Adaptive Autopilot Control Structure

Since the 3-DOF helicopter is underactuated, the motion along the roll and yaw axes has to be controlled simultaneously by one single input. The adaptive autopilot control structure, depicted in Fig 2, considers that the control input u_1 controls both roll and yaw dynamics, while the control input u_2 controls the pitch dynamics. Thus, it is necessary to design a control strategy to control the attitude of the system with only two control inputs. To achieve this, the roll and yaw trajectories are defined as a user defined input. The pitch trajectory is affected by both yaw and roll dynamics, and the desired trajectory for the pitch is calculated based on an internal loop. Define the virtual inputs v_1 and v_2 as

Castaneda et al. (2016),

$$v_1 = \cos \theta u_1 \tag{2a}$$

$$v_2 = \cos \epsilon \sin \theta u_1 \tag{2b}$$

which makes the dynamic equations (1) as,

$$J_\epsilon \ddot{\epsilon} = G \cos \epsilon + L_a v_1 \tag{3a}$$

$$J_\psi \ddot{\psi} = L_a v_2 \tag{3b}$$

$$J_\theta \ddot{\theta} = L_h u_2 \tag{3c}$$

Using (2), the input u_1 can be written as Castaneda et al. (2016),

$$u_1^2 = v_1^2 + \frac{v_2^2}{\cos^2 \epsilon} \tag{4}$$

The proposed autopilot is based on this fact: The decoupling can be carried out provided that the virtual inputs v_1 and v_2 given in (2) are satisfied. Then, the control u_1 can be expressed as,

$$u_1 = S \cdot \sqrt{v_1^2 + \frac{v_2^2}{\cos^2 \epsilon}} \tag{5}$$

where

$$S = \begin{cases} \text{sgn}(v_1), & \text{if } v_1 \neq 0 \\ 0, & \text{if } v_1 = 0 \end{cases}$$

Then, a way to decouple the system consists in forcing the angle θ , by the control input u_2 , to track the following desired trajectory,

$$\theta^*(t) = \tan^{-1} \frac{v_2}{\cos \epsilon v_1} \tag{6}$$

The control objective is to design a control law v_1 , v_2 , and u_2 to make the system’s states ϵ , ψ , and θ track their respective pre-defined time-dependent reference trajectories ϵ^* , ψ^* , and θ^* under the assumption of unknown parameters. In this paper, all parameters, M_h , M_w , L_a , L_w , L_h , g , J_ϵ , J_ψ , and J_θ are assumed to be unknown.

3 Adaptive Control Strategy

The control approach is based on a feedforward adaptive controller and a stabilizing feedback loop. The feedforward is designed to learn online the helicopter’s inverse dynamics through first-order reference models that define the desired errors dynamics. Due to the nature and high complexity order of the helicopter’s dynamical model, the adaptive controller may take a relatively long time to converge which may lead to an unstable or unsatisfactory performance. Therefore, a stabilizing feedback loop is designed to guarantee the system’s stability. The feedback loop can be viewed as a proportional-derivative compensator that stabilizes the system at start-up while the adaptive parameters are being updated. Additionally, it adds a disturbance rejection property to classical adaptive control that is known to suffer from unstructured uncertainties. Let $e_\epsilon = \epsilon - \epsilon^*$, $e_\psi = \psi - \psi^*$, and $e_\theta = \theta - \theta^*$ denote the system’s tracking errors. The control objective is to track these errors to zero. For that, let us define the following reference model:

$$s_\epsilon = \dot{e}_\epsilon + \eta_\epsilon e_\epsilon = \dot{\epsilon} - \dot{\epsilon}_r \tag{7a}$$

$$s_\psi = \dot{e}_\psi + \eta_\psi e_\psi = \dot{\psi} - \dot{\psi}_r \tag{7b}$$

$$s_\theta = \dot{e}_\theta + \eta_\theta e_\theta = \dot{\theta} - \dot{\theta}_r \tag{7c}$$

with $\dot{\bullet}_r = \dot{\bullet}^* - \eta_\bullet e_\bullet$ and η_\bullet being a positive constant that defines the desired bandwidth of the closed-loop system. The symbol \bullet can be ϵ , ψ , or θ . Formulation (3) can also be expressed as:

$$v_1 = \frac{1}{L_a} (J_\epsilon \ddot{\epsilon} - G \cos \epsilon) \tag{8a}$$

$$v_2 = \frac{1}{L_a} J_\psi \ddot{\psi} \tag{8b}$$

$$u_2 = \frac{1}{L_h} J_\theta \ddot{\theta} \tag{8c}$$

Therefore, the desired dynamics can be expressed by the following helicopter’s inverse dynamics regression model:

$$\frac{1}{L_a} (J_\epsilon \ddot{\epsilon}_r - G \cos \epsilon) = \Upsilon_\epsilon^T P_\epsilon \tag{9a}$$

$$\frac{1}{L_a} J_\psi \ddot{\psi}_r = \Upsilon_\psi^T P_\psi \tag{9b}$$

$$\frac{1}{L_h} J_\theta \ddot{\theta}_r = \Upsilon_\theta^T P_\theta \tag{9c}$$

where Υ_\bullet is a vector of known functions (regressor) and P_\bullet is a vector of unknown parameters defined as,

$$P_\epsilon = \begin{bmatrix} J_\epsilon & G \\ L_a & L_a \end{bmatrix} \tag{10a}$$

Table 1 Physical parameters of the helicopter

Parameter	Helicopter	Unit
Mass of helicopter (M_h)	1.42	kg
Mass of counterweight (M_w)	1.87	kg
Arm length (L_a)	0.66	m
Arm length for counterweight (L_w)	0.66	m
Distance between propellers (L_h)	0.17	m
Gravity (g)	9.81	m s ²
Inertia on roll axis (ϵ)	1.0348	kg m ²
Inertia on pitch axis (θ)	0.0451	kg m ²
Inertia on yaw axis (ψ)	1.0348	kg m ²

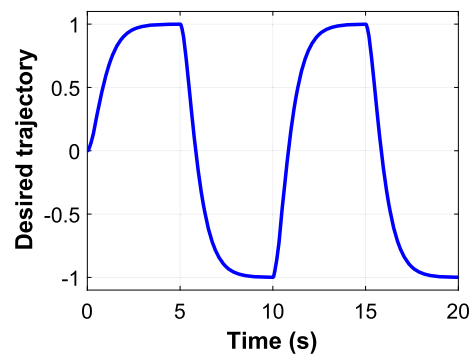


Fig. 3 Desired trajectory for all angles

$$P_\psi = \frac{J_\psi}{L_a} \tag{10b}$$

$$P_\theta = \frac{J_\theta}{L_h} \tag{10c}$$

Therefore, the control law is defined as,

$$v_1 = \Upsilon_\epsilon^T \hat{P}_\epsilon - K_\epsilon s_\epsilon \tag{11a}$$

$$v_2 = \Upsilon_\psi^T \hat{P}_\psi - K_\psi s_\psi \tag{11b}$$

$$u_2 = \Upsilon_\theta^T \hat{P}_\theta - K_\theta s_\theta \tag{11c}$$

where K_\bullet is a positive constant gain. The symbol $\hat{\bullet}$ denotes the estimate vector.

Theorem 1 Consider a nonlinear system in the form (1) with slowly time-varying parameters. Using the control law (11), the closed-loop system’s stability is guaranteed with the following adaptation law:

$$\dot{\hat{P}}_\epsilon = -\Gamma_\epsilon \Upsilon_\epsilon s_\epsilon \tag{12a}$$

$$\dot{\hat{P}}_\psi = -\Gamma_\psi \Upsilon_\psi s_\psi \tag{12b}$$

$$\dot{\hat{P}}_\theta = -\Gamma_\theta \Upsilon_\theta s_\theta \tag{12c}$$

where $\Gamma = [\gamma_1, \gamma_2, \dots, \gamma_m]^T$ and γ_i is a positive constant gain, $i = 1, \dots, m$.

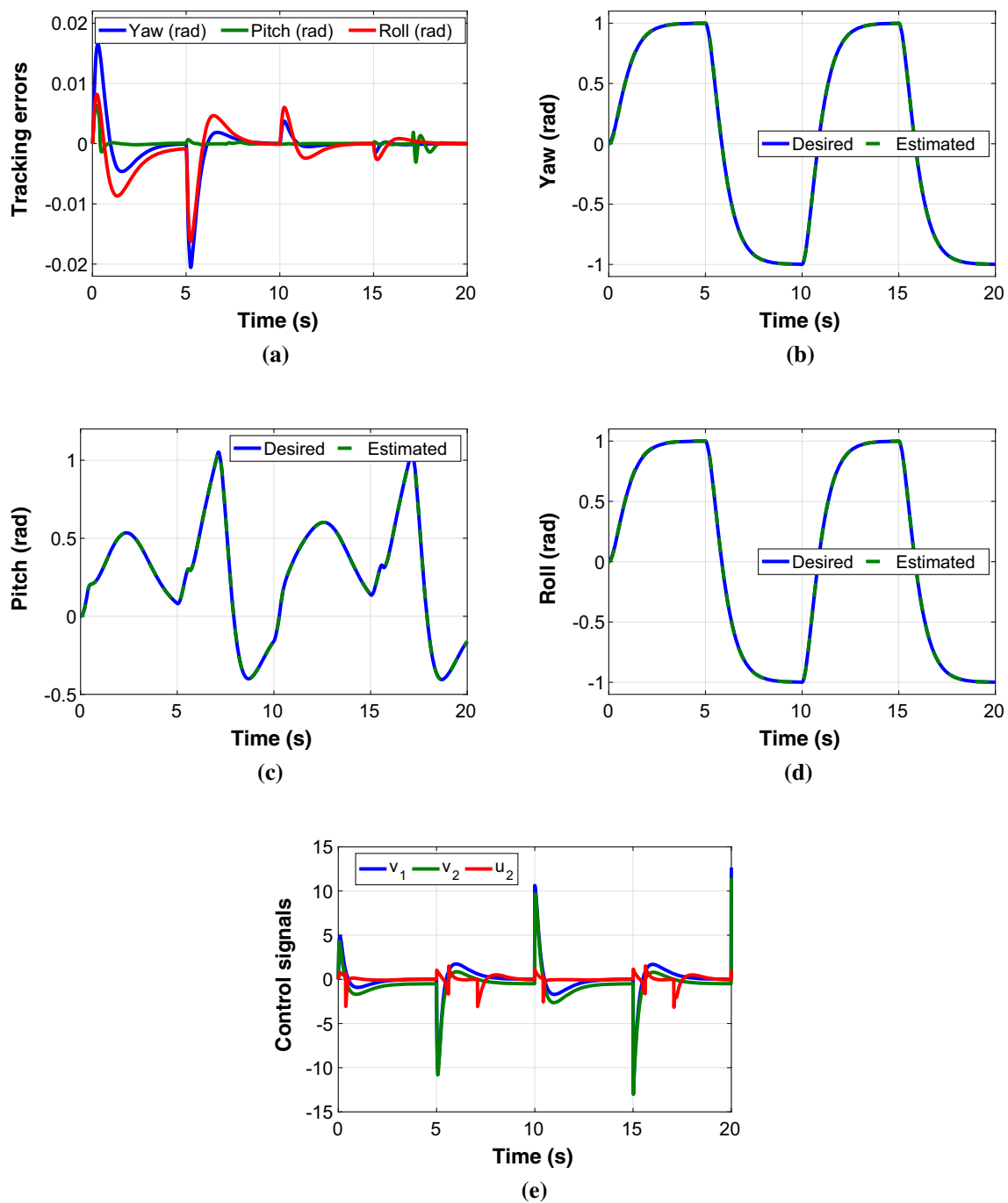


Fig. 4 Nominal case: **a** tracking errors; **b** yaw; **c** pitch; **d** roll; and **e** control signals

Proof Taking the time derivative of (7) yields,

$$\dot{s}_\epsilon = \ddot{\epsilon} - \ddot{\epsilon}_r \tag{13a}$$

$$\dot{s}_\psi = \ddot{\psi} - \ddot{\psi}_r \tag{13b}$$

$$\dot{s}_\theta = \ddot{\theta} - \ddot{\theta}_r \tag{13c}$$

Using (3) and the regression model (9) leads to,

$$\dot{s}_\epsilon = v_1 - \gamma_\epsilon^T P_\epsilon \tag{14a}$$

$$\dot{s}_\psi = v_2 - \gamma_\psi^T P_\psi \tag{14b}$$

$$\dot{s}_\theta = u_2 - \gamma_\theta^T P_\theta \tag{14c}$$

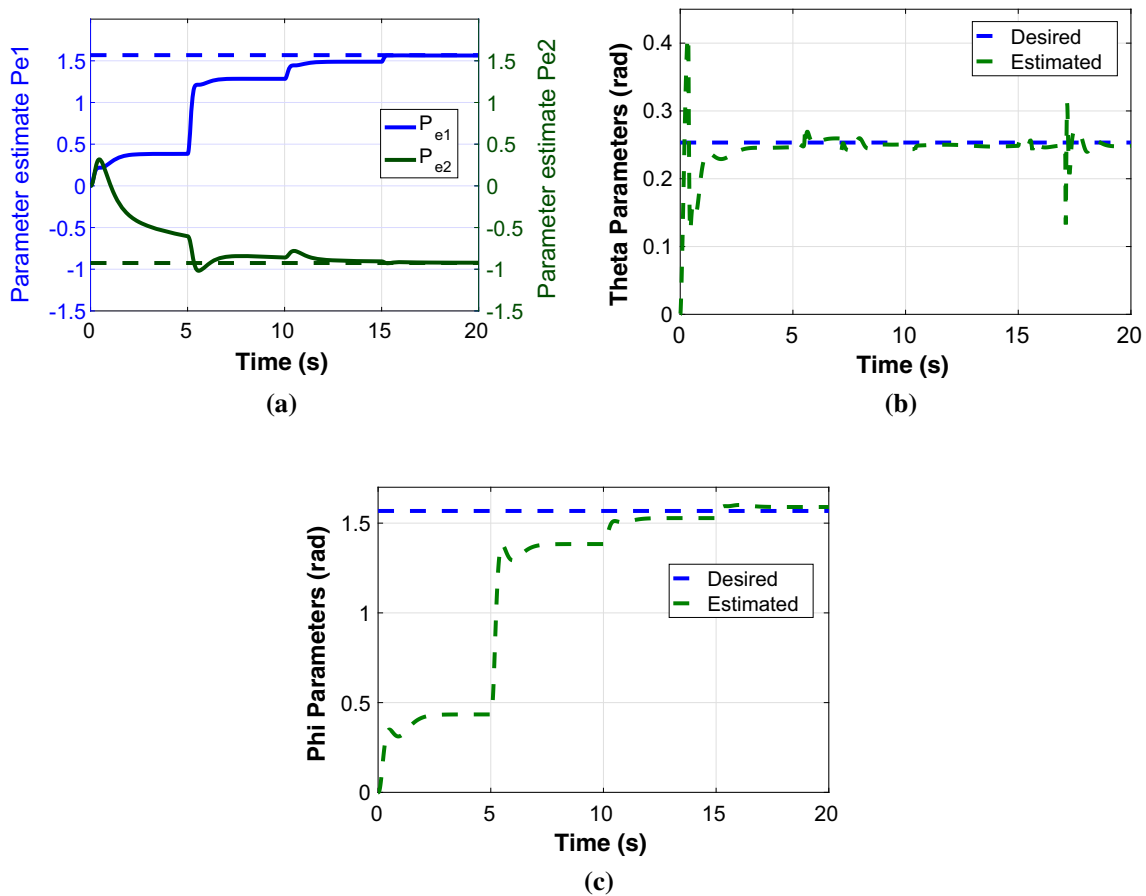


Fig. 5 Parameter estimation: a \hat{P}_ϵ ; b \hat{P}_θ ; and c \hat{P}_ψ

Consider a Lyapunov candidate as follows:

$$V = \frac{1}{2} \{s_\epsilon^2 + s_\psi^2 + s_\theta^2 + \tilde{P}_\epsilon^T \Gamma_\epsilon^{-1} \tilde{P}_\epsilon + \tilde{P}_\psi^T \Gamma_\psi^{-1} \tilde{P}_\psi + \tilde{P}_\theta^T \Gamma_\theta^{-1} \tilde{P}_\theta\}$$

Take the time derivative of V :

$$\dot{V} = \dot{s}_\epsilon s_\epsilon + \dot{s}_\psi s_\psi + \dot{s}_\theta s_\theta + \tilde{P}_\epsilon^T \Gamma_\epsilon^{-1} \dot{\tilde{P}}_\epsilon + \tilde{P}_\psi^T \Gamma_\psi^{-1} \dot{\tilde{P}}_\psi + \tilde{P}_\theta^T \Gamma_\theta^{-1} \dot{\tilde{P}}_\theta$$

The variation of parameters P_\bullet is assumed to be negligible compared to the system’s time constants, i.e., $\dot{P}_\bullet = \dot{\tilde{P}}_\bullet$. Substitute \dot{s}_ϵ , \dot{s}_ψ , and \dot{s}_θ from (14):

$$\dot{V} = \{v_1 - \gamma_\epsilon^T P_\epsilon\} s_\epsilon + \{v_2 - \gamma_\psi^T P_\psi\} s_\psi + \{u_2 - \gamma_\theta^T P_\theta\} s_\theta + \tilde{P}_\epsilon^T \Gamma_\epsilon^{-1} \dot{\tilde{P}}_\epsilon + \tilde{P}_\psi^T \Gamma_\psi^{-1} \dot{\tilde{P}}_\psi + \tilde{P}_\theta^T \Gamma_\theta^{-1} \dot{\tilde{P}}_\theta$$

Setting the control law as in (11) leads to,

$$\dot{V} = \gamma_\epsilon^T \tilde{P}_\epsilon s_\epsilon + \gamma_\psi^T \tilde{P}_\psi s_\psi + \gamma_\theta^T \tilde{P}_\theta s_\theta$$

$$+ \tilde{P}_\epsilon^T \Gamma_\epsilon^{-1} \dot{\tilde{P}}_\epsilon + \tilde{P}_\psi^T \Gamma_\psi^{-1} \dot{\tilde{P}}_\psi + \tilde{P}_\theta^T \Gamma_\theta^{-1} \dot{\tilde{P}}_\theta - K_\epsilon s_\epsilon^2 - K_\psi s_\psi^2 - K_\theta s_\theta^2$$

where $\tilde{P}_\bullet = \hat{P}_\bullet - P_\bullet$. Setting the adaptation law as in (12) implies that,

$$\dot{V} = -K_\epsilon s_\epsilon^2 - K_\psi s_\psi^2 - K_\theta s_\theta^2 < 0 \quad \forall K_\bullet > 0$$

Setting $K_\bullet > 0$ yields $\dot{V} < 0, \forall s_\bullet \neq 0$ so that $s_\bullet = 0$ is a globally asymptotically stable equilibrium point. A positive Lyapunov function V , which is decreasing ($\dot{V} < 0$), must converge to a finite limit. Therefore, the system is asymptotically stable in the sense of Lyapunov. Hence, signals $s_\bullet, \tilde{P}_\bullet$, and \hat{P}_\bullet are also bounded and converge to finite values. It follows from (7) that e_\bullet and \dot{e}_\bullet are bounded, which implies from (14) that \dot{s}_\bullet is also bounded. \square

For non-autonomous systems, finding a Lyapunov function V with a negative definite derivative ($\dot{V} < 0$) does not lead to a conclusion about the asymptotic stability. Therefore, Barbalat’s lemma is applied for the time-varying system in hand to prove its asymptotic stability and convergence.

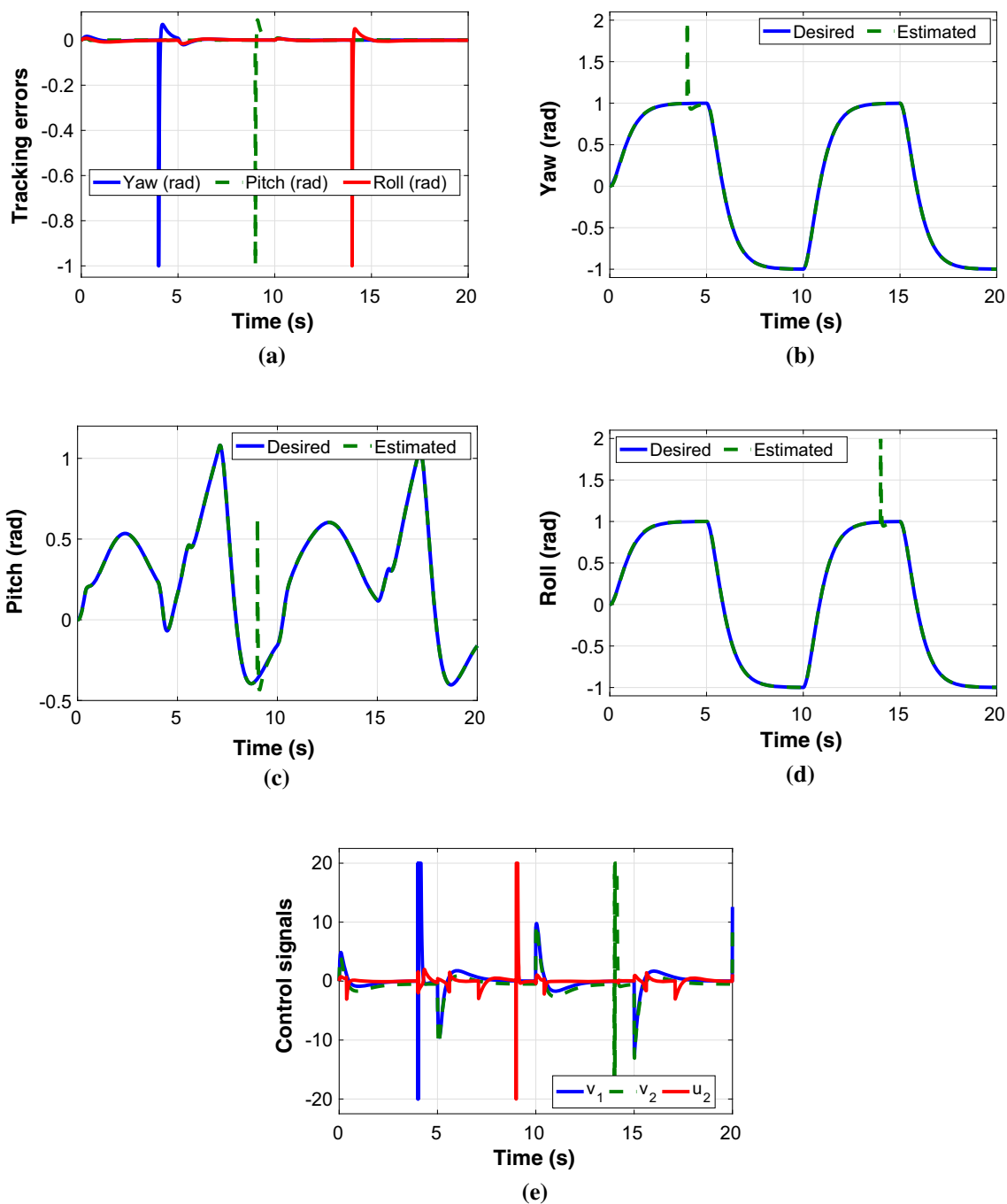


Fig. 6 Disturbances added: **a** tracking errors; **b** yaw; **c** pitch; **d** roll; and **e** control signals

Lemma 1 (Barbalat) *If the differentiable function $V(t)$ has a finite limit as $t \rightarrow \infty$, and if $\dot{V}(t)$ is uniformly continuous, then $\dot{V}(t) \rightarrow 0$ as $t \rightarrow \infty$.*

Taking the derivative of \dot{V} yields,

$$\ddot{V} = -2(K_\epsilon \dot{s}_\epsilon s_\epsilon + K_\psi \dot{s}_\psi s_\psi + K_\theta \dot{s}_\theta s_\theta)$$

Therefore, \ddot{V} is also bounded.

From Lemma 1, V has a finite limit as $t \rightarrow \infty$ and \dot{V} is uniformly continuous. Therefore, $\lim_{t \rightarrow \infty} \dot{V} = 0$, and hence, $\lim_{t \rightarrow \infty} s_\bullet = 0$. Therefore, $\lim_{t \rightarrow \infty} e_\bullet = 0$ and $\lim_{t \rightarrow \infty} \dot{e}_\bullet = 0$.

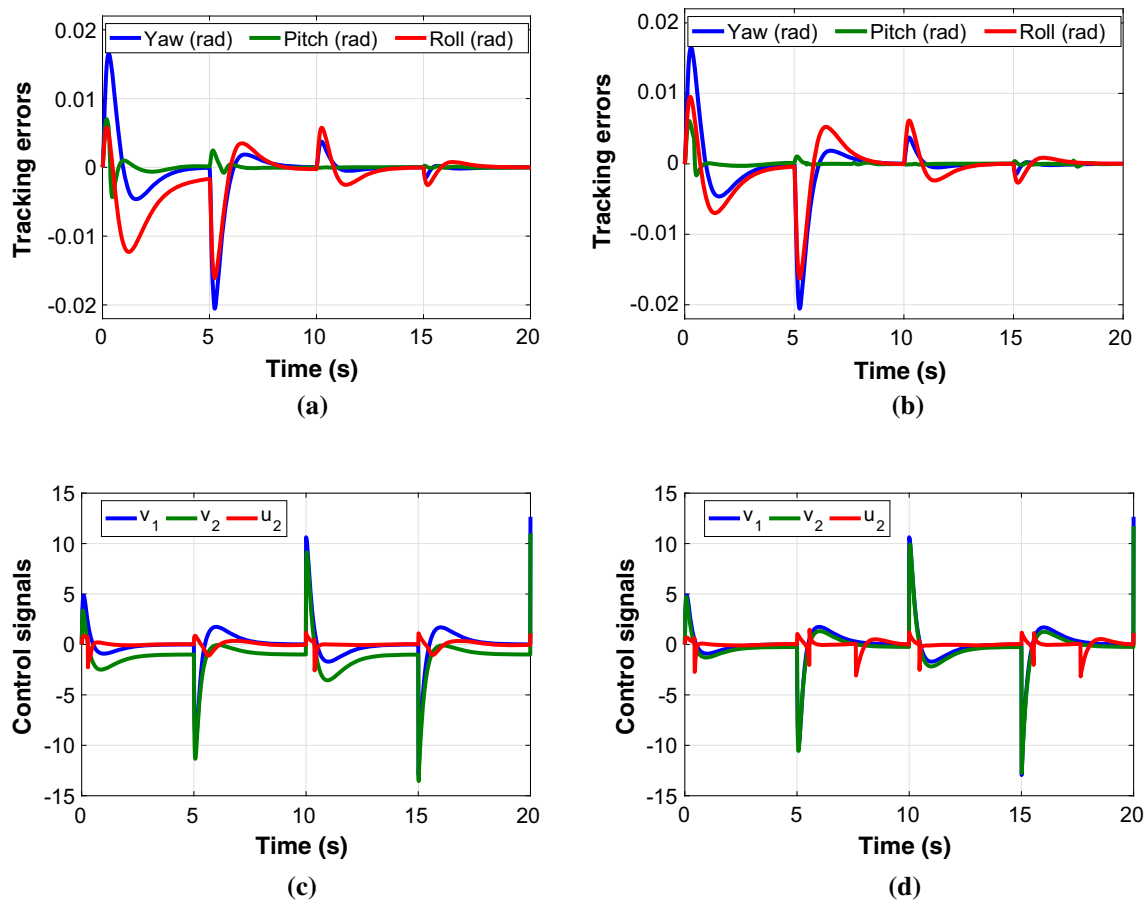


Fig. 7 Tracking errors under parameters change: **a** doubled mass; **b** half mass; **c** control signals for doubled mass; and **d** control signals for half mass

4 Results and Discussion

4.1 Setup

Different tests are performed to show the effectiveness of the proposed scheme. Table 1 summarizes the physical parameters of the helicopter along with their respective values. The control coefficients are set to $\eta_\epsilon = 40$, $\eta_\psi = 12$, $\eta_\theta = 16$, $K_\epsilon = 25$, $K_\psi = 2.5$, $K_\theta = 3$, $\Gamma_\epsilon = [4.5 \times 10^{-2}, 0.3]^T$, $\Gamma_\psi = 8 \times 10^{-3}$, $\Gamma_\theta = 5 \times 10^{-2}$, and the gravitational constant is set to $g = 9.8 \text{ m/s}^2$. The controller is set to operate at a sampling frequency of 100 Hz. The desired position reference trajectory is considered as a sequence of step responses of a critically damped second-order system with a natural frequency $\omega_n = 2 \text{ rad/s}$, as illustrated in Fig. 3. The system's response is studied taking into account the helicopter's angles. To better show the convergence properties of the adaptive controller, all adaptive parameters \hat{P}_\bullet are initially set to zero. It is important to note that the desired values of \hat{P}_\bullet are calculated using (10) and the physical parameters of the helicopter in Table 1.

4.2 Results

4.2.1 Nominal Case

The system's response is studied taking into account the helicopter's tracking errors e_\bullet and the adaptive parameters \hat{P}_\bullet , and the control signals v_1 , v_2 , and u_2 . First, the proposed adaptive control scheme is tested on the helicopter in the nominal case. Results are shown in Fig. 4. As it is shown, the motion tracking errors converge gradually to zero after each reference trajectory change. On the other hand, parameter estimation performance is depicted in Fig. 5. The adaptive parameters show good convergence to their nominal values. The ability of the proposed controller in dealing with parametric uncertainties is clearly demonstrated.

4.2.2 Effect of Disturbances

To show the robustness of the controller against unstructured uncertainties, unexpected sudden step disturbances are introduced to the system. For that, a step disturbance of 1 rad is added to the yaw, pitch, and roll axes at time 4 s, 9 s, and 14 s,

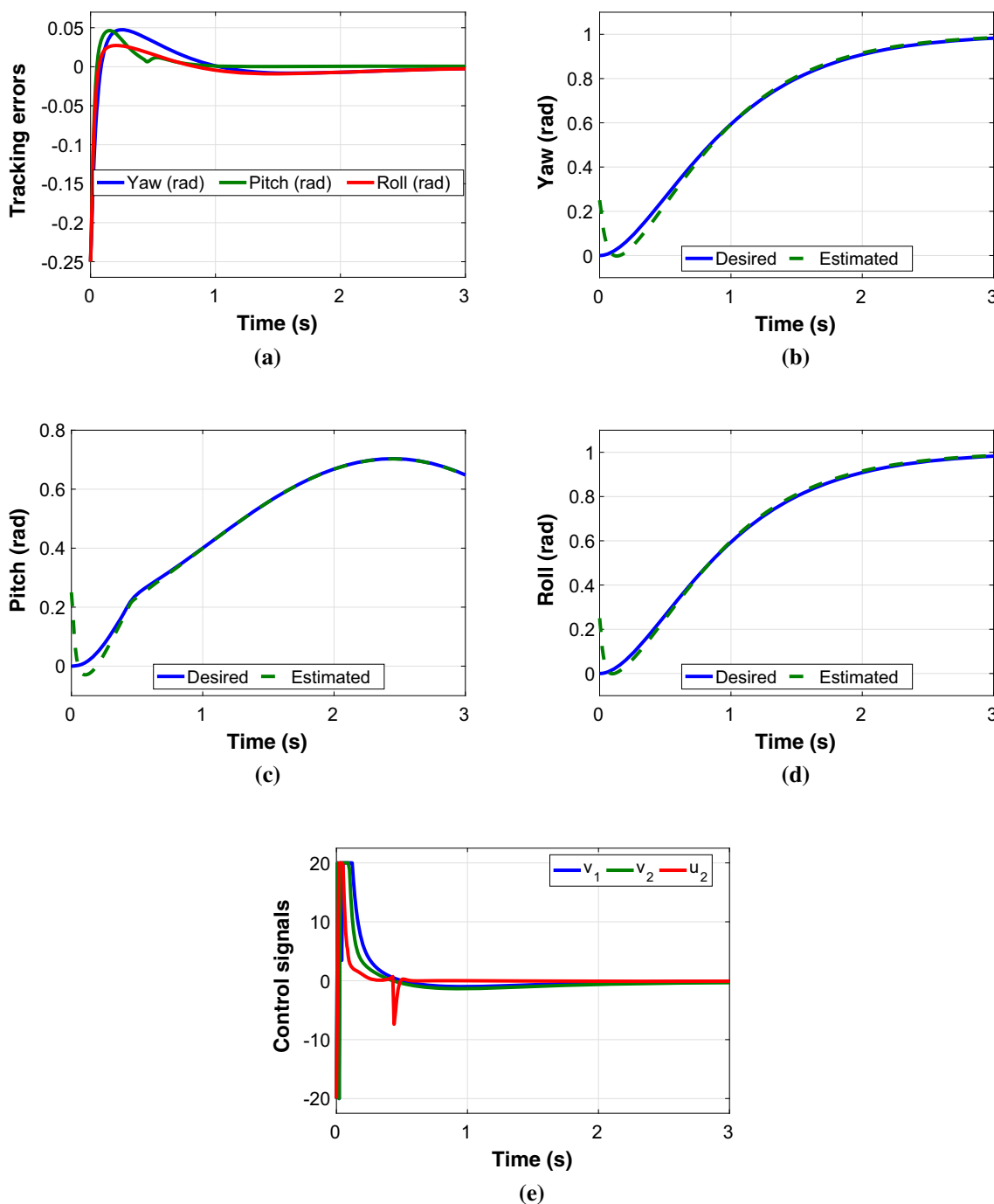


Fig. 8 Nonzero initial conditions: **a** tracking errors; **b** yaw; **c** pitch; and **d** roll; **e** control signals

respectively. Results reported in Fig. 6 show that even under the disturbances the controller is efficient in decaying the errors to approximately zero without significant overshoot or oscillations. It is noteworthy the saturation of control signals at ± 20 as shown in Fig. 6e. The advantage behind the use of such controller is revealed by this test.

4.2.3 Effect of Parameter Variations

To further show the effectiveness of the controller under the parametric uncertainties, the mass of the system is changed by a factor of two and in another case by half. Similar to the nominal case, the tracking errors depicted in Fig. 7 show that controller is able to get the tracking errors to converge to zero even in the presence of parametric uncertainties. This is

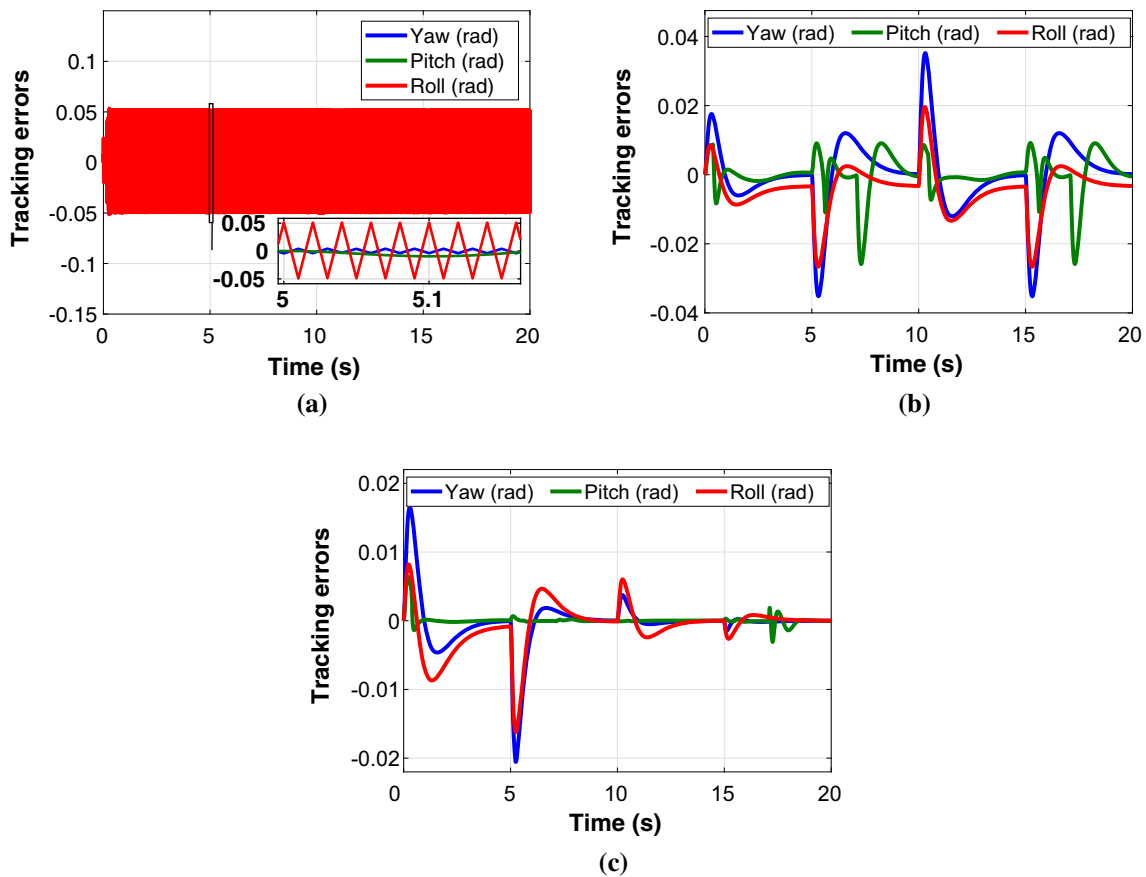


Fig. 9 Comparison: **a** adaptive SMC; **b** PID control; and **c** adaptive control

Table 2 Performance comparison

	Proposed method	PID control	Adaptive SMC
σ_e	0.05	0.40	0.76
σ_c	1.4×10^4	1.4×10^4	2.3×10^4

expected since no a priori parameters knowledge is required by the controller even in the nominal case. Thus, the proposed controller is instrumental in achieving the needed robustness against parametric uncertainties.

4.2.4 Effect of Nonzero Initial Conditions

To study the effect of initial conditions on the proposed controller, an initial condition of ($\epsilon = \psi = \theta = 0.25$) rad is introduced. Results, depicted in Fig. 8, are shown for 3s to better show the convergence properties of the system. The controller provides a satisfactory transient response. All angles converge quickly to their desired trajectories. Figure 8e shows control signals raising saturation and decreasing gradually as the initial tracking errors are minimized.

4.2.5 Comparison Against Other Control Methods

The proposed adaptive control scheme is compared against a conventional PID controller and the adaptive sliding-mode controller (SMC) presented in Li et al. (2015b). The tracking errors are shown in Fig. 9. It is clearly shown that unlike sliding-mode control, the proposed adaptive controller is able to bring the tracking errors to zero over time. In principle, sliding mode is achieved by discontinuous control and switching at infinite frequency. However, switching frequency is limited in real-life applications and results in discretization chattering problem as it is illustrated in Fig. 9. To overcome this problem, the boundary solution can be used to replace the discontinuous control by a saturation function that approximates the sign function in a boundary layer of sliding-mode manifold. This solution preserves partially the invariance property of sliding mode where states are confined to a small vicinity of the manifold, and convergence to zero cannot be guaranteed because robustness to parameter variations and uncertain disturbances is obtained only when sliding mode truly occurs. Similarly, the PID controller is able to decay the tracking errors to a magnitude within the range obtained by the adaptive SMC. It is important to

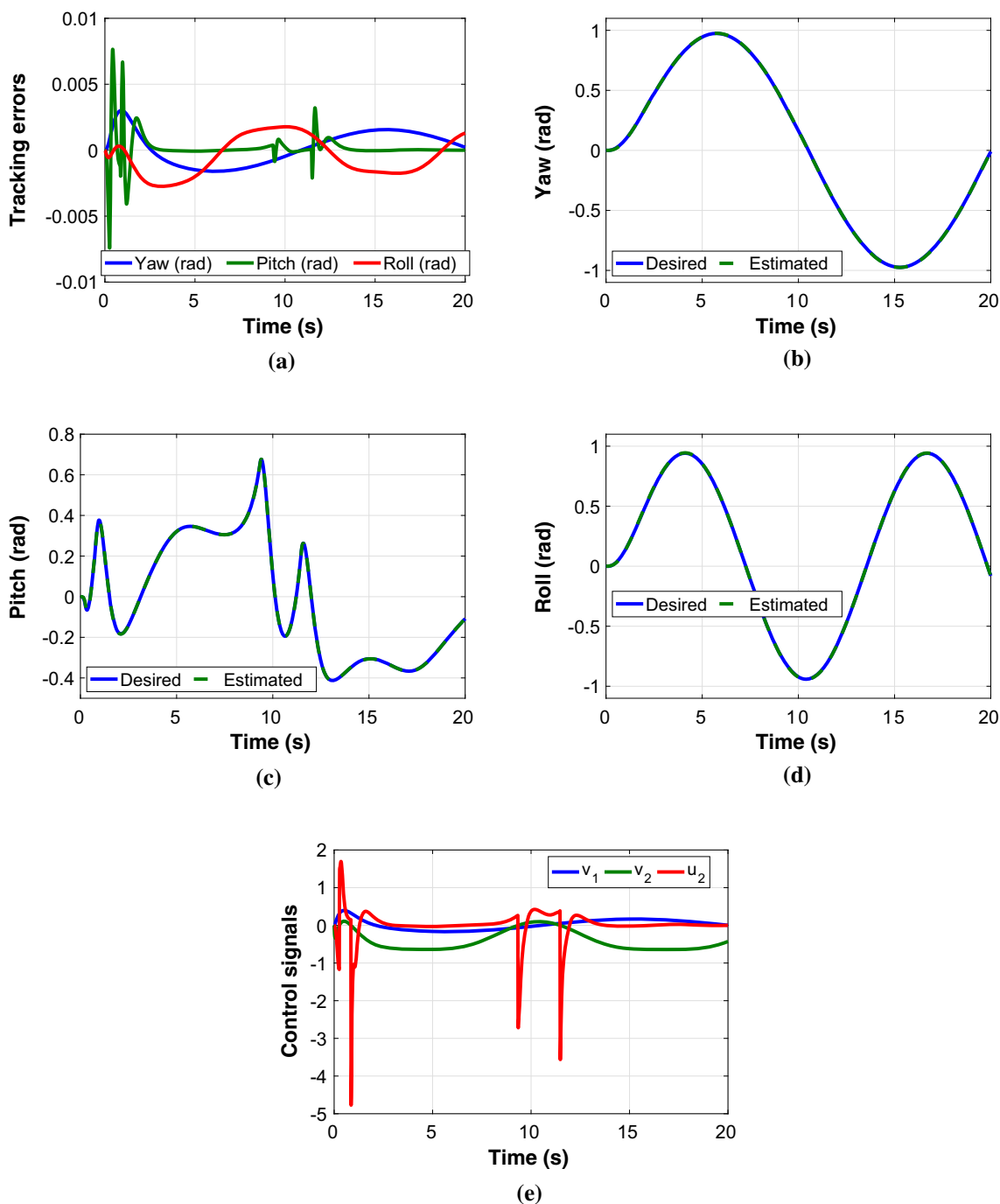


Fig. 10 Sine-wave trajectory: **a** tracking errors; **b** yaw; **c** pitch; **d** roll; and **e** control signals

note that tracking errors under PID control and the proposed control scheme have a similar initial magnitude; but, only the adaptive controller is able to decrease the magnitude of these errors further as parameters converge to their desired values.

To quantitatively adjudge the trajectory tracking performance, two performance metrics are introduced. First, the integral of the tracking error σ_e is calculated over a single

run. The second performance index σ_c consists of the integral of the control signals. These metrics are calculated as follows:

$$\sigma_e = \int_{t_0}^{t_f} (e_\epsilon^2 + e_\psi^2 + e_\theta^2) dt \tag{15a}$$

$$\sigma_c = \int_{t_0}^{t_f} (v_1^2 + v_2^2 + u_2^2) dt \tag{15b}$$

where t_0 and t_f are initial and final time instants, respectively. The obtained numerical values for both performance metrics are displayed in Table 2. The proposed adaptive control method yields the lowest tracking performance index with a control effort equal to that of the PID controller. The adaptive SMC achieves the highest tracking performance index and control effort.

4.2.6 Effect of Other Reference Trajectories

Finally, the proposed adaptive controller is validated using different reference trajectories. For that, a 0.33 rad/s and 0.5 rad/s sine-wave trajectories are, respectively, set to the yaw and roll. Results are depicted in Fig. 10. Regardless of the trajectory, the proposed controller tracks all trajectories with high precision.

5 Conclusion

In this paper, a Lyapunov-based adaptive controller is proposed for high-performance control of a 3-DOF helicopter. The controller learns over time the system's inverse model while also coping with unstructured uncertainties. As such, the control scheme achieves asymptotic convergence and tracking by a Lyapunov-based adaptation law in the presence of both structured and unstructured uncertainties. Unlike other controllers, no a priori parameters knowledge is required and the system's closed-loop stability is guaranteed by Lyapunov direct method. The controller is tested under different conditions to evaluate its robustness properties in the presence of various uncertainties. Results show that the helicopter's motion can be tracked with high accuracy. Henceforth, the adaptive control approach can be extended to improve static and dynamic performance of high-performance motion systems. As a future work, a comparative study against various advanced control schemes can be envisioned along with physical implementation.

References

- Boby, R. I., Mansor, H., Gunawan, T. S., & Khan, S. (2014). Robust adaptive LQR control of nonlinear system application to 3-DOF flight control system. In *International conference on smart instrumentation, measurement and applications*, IEEE.
- Castaneda, H., Plestan, F., Chriette, A., & de Leon-Morales, J. (2016). Continuous differentiator based on adaptive second-order sliding-mode control for a 3-DOF helicopter. *IEEE Transactions on Industrial Electronics*, 63(9), 5786–5793.
- Chaoui, H., & Gueaieb, W. (2008). Type-2 fuzzy logic control of a flexible-joint manipulator. *Journal of Intelligent and Robotic Systems*, 51(2), 159–186.
- Chaoui, H., & Sicard, P. (2012a). Neural network modeling of cold-gas thrusters for a spacecraft formation flying test-bed. In *IEEE conference on industrial electronics society* (pp. 2619–2621).
- Chaoui, H., & Sicard, P. (2012b). Adaptive fuzzy logic control of permanent magnet synchronous machines with nonlinear friction. *IEEE Transactions on Industrial Electronics*, 59(2), 1123–1133.
- Chen, M., Shi, P., & Lim, C. C. (2016). Adaptive neural fault-tolerant control of a 3-DOF model helicopter system. *IEEE Transactions on Systems, Man, and Cybernetics: Systems*, 46(2), 260–270.
- Coza, C., & Macnab, C. (2006). A new robust adaptive-fuzzy control method applied to quadrotor helicopter stabilization. In *Annual meeting of the North American Fuzzy Information Processing Society (NAFIPS)* (pp. 454–458).
- Cruz, S. S., Kendoul, F., Lozano, R., & Fantoni, I. (2008). Real-time stabilization of a small three-rotor aircraft. *IEEE Transactions on Aerospace and Electronic Systems*, 44(2), 783–794.
- Dierks, T., & Jagannathan, S. (2010). Output feedback control of a quadrotor UAV using neural networks. *IEEE Transactions on Neural Networks*, 21(1), 50–66.
- Du, Y., Fang, J., & Miao, C. (2014). Frequency-domain system identification of an unmanned helicopter based on an adaptive genetic algorithm. *IEEE Transactions on Industrial Electronics*, 61(2), 870–881.
- Dube, D. Y., & Patel, H. G. (2016). Control design of 3 DOF helicopter system. In *International conference on industrial and information systems* (pp. 247–252).
- Efe, M. O. (2011). Neural network assisted computationally simple PI lambda D mu control of a quadrotor UAV. *IEEE Transactions on Industrial Informatics*, 7(2), 354–361.
- Fradkov, A. L., Andrievsky, B., & Peaucelle, D. (2010). Estimation and control under information constraints for LAAS helicopter benchmark. *IEEE Transactions on Control Systems Technology*, 18(5), 1180–1187.
- Gao, W. N., & Fang, Z. (2012). Adaptive integral backstepping control for a 3-DOF helicopter. In *International conference on information and automation* (pp. 190–195).
- Guo, Y., Zheng, Z., Zhu, M., & Wu, Z. (2016). Neural network tracking control of the 3-DOF helicopter with input saturation. In *Chinese control and decision conference IEEE* (pp. 2656–2660).
- Khayamy, M., Chaoui, H., Oukaour, A., & Gualous, H. (2016). Adaptive fuzzy logic control mixing strategy of DC/DC converters in both discontinuous and continuous conduction modes. *Journal of Control, Automation and Electrical Systems*, 7(3), 274–288.
- Kocagil, B. M., Ozcan, S., Arican, A. C., Guzey, U. M., Copur, E. H., & Salamci, M. U. (2018). MRAC of a 3-DOF helicopter with nonlinear reference model. In *Mediterranean conference on control and automation*, IEEE (pp. 278–283).
- Kutay, A. T., Calise, A. J., Idan, M., & Hovakimyan, N. (2005). Experimental results on adaptive output feedback control using a laboratory model helicopter. *IEEE Transactions on Control Systems Technology*, 13(2), 196–202.
- Li, Z., Liu, H. H. T., Zhu, B., & Gao, H. (2015a). Robust second-order consensus tracking of multiple 3-DOF laboratory helicopters via output feedback. *IEEE/ASME Transactions on Mechatronics*, 20(5), 2538–2549.
- Li, Z., Liu, H. H. T., Zhu, B., Gao, H., & Kaynak, O. (2015b). Nonlinear robust attitude tracking control of a table-mount experimental helicopter using output feedback. *IEEE Transactions on Industrial Electronics*, 62(9), 5665–5676.
- Li, C., Quan, K., Xiao, B., & Yang, X. (2017). Adaptive fuzzy-based backstepping control of a 3-DOF helicopter testbed with dead-zone. In *International conference on advanced mechatronic systems* (pp. 208–2013).
- Liu, H., Lu, G., & Zhong, Y. (2013). Robust LQR attitude control of a 3-DOF laboratory helicopter for aggressive maneuvers. *IEEE Transactions on Industrial Electronics*, 60(10), 4627–4636.

- Marantos, P., Bechlioulis, C. P., & Kyriakopoulos, K. J. (2017). Robust trajectory tracking control for small-scale unmanned helicopters with model uncertainties. *IEEE Transactions on Control Systems Technology*, 25(6), 2010–2021.
- Pedro, J. O., & Kala, P. J. (2015). Nonlinear control of quadrotor UAV using Takagi–Sugeno fuzzy logic technique. In *IEEE control conference (ASCC), 2015 10th Asian* (pp. 1–6).
- Rajappa, S., Chriette, A., Chandra, R., & Khalil, W. (2013). Modeling and dynamic identification of 3 DOF Quanser helicopter. In *IEEE/RSJ international conference on intelligent robots and systems*.
- Tanaka, K., Ohtake, H., & Wang, H. O. (2004). A practical design approach to stabilization of a 3-DOF RC helicopter. *IEEE Transactions on Control Systems Technology*, 12(2), 315–325.
- Veeraboina, A. K., & Ordonez, R. (2018). Design and implementation of linear/nonlinear control methods on 3-DOF helicopter. In *IEEE national aerospace and electronics conference*, IEEE (pp. 435–442).
- Xian, B., Guo, J., & Zhang, Y. (2015). Adaptive backstepping tracking control of a 6-DOF unmanned helicopter. *IEEE/CAA Journal Of Automatica Sinica*, 2(1), 19–24.
- Zheng, B., & Zhong, Y. (2011). Robust attitude regulation of a 3-DOF helicopter benchmark theory and experiments. *IEEE Transactions on Industrial Electronics*, 58(2), 660–670.
- Zou, Y., & Zheng, Z. (2015). A robust adaptive RBFNN augmenting backstepping control approach for a model-scaled helicopter. *IEEE Transactions on Control Systems Technology*, 23(6), 2344–2352.

Publisher's Note Springer Nature remains neutral with regard to jurisdictional claims in published maps and institutional affiliations.